BMC Plant Biology

RESEARCH

Open Access

Characterizing seed dormancy in *Epimedium brevicornu* Maxim.: Development of novel chill models and determination of dormancy release mechanisms by transcriptomics

Pengshu Li[1,3], Qiuyan Xiang[1], Yue Wang[2*] and Xuehui Dong[1*]

Abstract

Purpose *Epimedium brevicornu* Maxim. is a perennial persistent C3 plant of the genus *Epimedium* Linn. in the family *Berberaceae* that exhibits severe physiological and morphological seed dormancy.We placed mature *E. brevicornu* seeds under nine stratification treatment conditions and explored the mechanisms of influence by combining seed embryo growth status assessment with related metabolic pathways and gene co-expression analysis.

Results We identified 3.9 °C as the optimum cold-stratification temperature of *E. brevicornu* seeds via a chilling unit (CU) model. The best treatment was variable-temperature stratification (10/20 °C, 12/12 h) for 4 months followed by low-temperature stratification (4 °C) for 3 months (4-3). A total of 63801 differentially expressed genes were annotated to 2587 transcription factors (TFs) in 17 clusters in nine treatments (0-0, 0-3, 1-3, 2-3, 3-3, 4-3, 4-2, 4-1, 4-0). Genes specifically highly expressed in the dormancy release treatment group were significantly enriched in embryo development ending in seed dormancy and fatty acid degradation, indicating the importance of these two processes. Coexpression analysis implied that the TF GRF had the most reciprocal relationships with genes, and multiple interactions centred on zf-HD and YABBY as well as on MYB, GRF, and TCP were observed.

Conclusion In this study, analyses of plant hormone signal pathways and fatty acid degradation pathways revealed changes in key genes during the dormancy release of *E. brevicornu* seeds, providing evidence for the filtering of *E. brevicornu* seed dormancy-related genes.

Keywords *Epimedium brevicornu* Maxim., Seed dormancy, Chill models, RNA-Seq

Introduction

Epimedium brevicornu Maxim. is an important perennial medicinal plant, its dry leaves have been recorded in the Chinese Pharmacopoeia (2020), called EPIMEDII FOLIUM. Icaritin is the main active ingredient present in EPIMEDII FOLIUM, which offers a range of health benefits, such as immune regulation, anti-inflammatory, anti-aging and anti-tumor [1]. The annual demand for EPIMEDII FOLIUM is approximately 3500 tons, which is increasing annually [2]. In the past five years, its market price has been increased from 45 China Yuan (CNY)

*Correspondence:
Yue Wang
yuesupermax@163.com
Xuehui Dong
b20223010107@cau.edu.cn
[1] College of Agronomy and Biotechnology, China Agricultural University, No. 2, Old Summer Palace West Road, Haidian District, Beijing 100193, China
[2] Shandong Academy of Agricultural Sciences, Jinan 250100, Shandong, China
[3] College of Agronomy and Biotechnology, Sanya Institute of China Agricultural University, Sanya 610101, Hainan, China

to approximately 140 CNY per kilogram. *E. brevicornu* mainly came from the wild in the past, and artificial cultivation has just started. Seeds are the basic materials for artificial propagation, which is of great importance. Due to the considerable market demand and high price, the wild resources of *E. brevicornu* were faced with depletion due to excessive manual mining, and the resource availability became concerning. However, severe seed dormancy occurs during artificial cultivation, harvested seeds of *E. brevicornu* germinate approximately one year after sowing under natural conditions.

The seed is an important stage in the higher plant life cycle with respect to its survival as a species [3]. The seed enters a dormant state to optimize germination over time. Physiological dormancy (PD) seeds are water-permeable and have a fully developed embryo with a physiological inhibiting mechanism that prevents radicle emergence, morphological dormancy (MD) seeds have an underdeveloped embryo that needs to grow before germination, morphophysiological dormancy (MPD) seeds contain an underdeveloped embryo that is physiologically dormant [4]. According to previous research in our lab, embryos of newly harvested *E. brevicornu* seeds are usually undifferentiated and need more than 6 months for embryo maturation under natural conditions [5]. Based on the classification theory of seed dormancy, *E. brevicornu* seeds exhibit MPD [6, 7]. This dormancy has been a limit for large-scale artificial cultivation of *E. brevicornu*.

Stratification is a common method to release seed dormancy, but the optimum temperature varies with the dormancy stage. Low-temperature stratification can overcome endosperm inhibition and improve the growth of seed embryos [8]. However, variable-temperature stratification can improve the consistency of seed germination during low-temperature stratification, and the promotional effect is proportional to the length of variable-temperature stratification [9]. Seed dormancy depends on a network of signalling pathways integrated by the environment and multiple hormones. White spruce (*Picea glauca*) seeds showed significant changes in abscisic acid (ABA), gibberellin (GA) and indole-3-acetic acid (IAA) levels during moist chilling stratification, with significant upregulation of the transcript expression of transport inhibitor response 1 (TIR1), auxin response factor 4 (ARF4) and auxin/indole-3-acetic acid (Aux/IAA), which are components of the growth hormone signalling pathway; these changes mediate the dormancy release of white spruce seeds [10]. Ma et al. [11] used RNA-seq to examine dormancy release in *Epimedium pseudowushanense* B.L. Guo seeds by searching for candidate genes involved in the metabolism and signal transduction of ABA and GAs, which is important for the study of the physiological and morphological dormancy mechanisms of Epimedium seeds. The results showed that EpNCED1, EpNCED2, EpCYP707A1, and EpCYP707A2 may be involved in ABA biosynthesis and catabolism; that EpSnRK2 may be related to ABA signalling during seed dormancy; that EpGA3ox may be involved in GA biosynthesis; and that EpDELLA1 and EpDELLA2 may be related to GA signalling pathways.

Glucose promotes cell division, while sucrose is associated with cell maturation and starch synthesis, and the sugar-responsive pathway usually interacts with the phytohormone pathway [12]. Changes in seed embryo morphology undoubtedly alter the cell wall, and the main component of hemicellulose in the dicotyledon cell wall is xyloglucan. Xyloglucan endotransglycosylases (XETs) incorporate newly synthesized xyloglucan during xylem and phloem cell growth to control cell wall dissolution, loosening, and cell expansion [13]. In Arabidopsis, TCH4 has been identified as an XET that responds to regulation by brassinosteroids (BRs) to control cell expansion [14]. One of the major components of the endosperm cell wall in cereal seeds is β-1,3-glucan, and endosperm weakening is a major feature of endosperm expansion leading to endosperm rupture [15]. During seed germination in tobacco and tomato, weakening around the endosperm tip is closely associated with β-1,3-glucanase (EGLC), which causes additional physical dormancy of the testa, and the promoter of this enzyme-encoding gene is controlled by ABA [16, 17]. In addition, it has also been shown that GAs induce the expression of expansin (EXP) and members of the XET/XTH family to increase the growth potential of the seed embryo and weaken the mechanical restraint of the testa and endosperm covering the radicle to allow seed germination [18]. Thus, eventual cell wall disintegration and endosperm weakening to allow seed germination may require the action of several enzymes.

Transcription factors (TFs) are major regulatory proteins with sequence-specific DNA- or nucleotide-binding activity that play key roles in gene regulation during plant development. Their roles are mediated by interactions with cis-elements and/or other TFs and lead to the regulation of downstream genes at various developmental stages or during cellular responses to environmental factors [19, 20]. R2R3-MYB is a putative seed germination regulator involved in plant metabolism, development, and abiotic stress [21]. The interaction between MYB and bri1-ethyl methanesulphonate suppressor 1 (BES1) in Arabidopsis promotes BR target gene expression, allowing amplification of the BR signal [22]. In addition, the interaction between MYB77 and ARF7 is involved in regulating the growth hormone response, leading to a significant reduction in the number of lateral roots in plants, and the interaction between MYB

and HFR1 assists in the accumulation of phytochrome A (phyA), which plays a role in seedling growth [23, 24]. Transferase complex subunit pseudogene (TCP) has been shown to be a key player in the biosynthesis of lipids and phytohormones, such as BRs and jasmonate (JA), and to control seed germination [25–27]. Loss of function of knotted-related homeobox (KNOX) resulting in reduced 18:2ω-hydroxy fatty acid in the seed cutin alters cuticle layer permeability and has been shown to help regulate physical seed dormancy in *M. truncatula* L. and mungbean (*Vigna radiata* [L.] Wilczek) [28]. The interaction between KNOX and growth-regulating factor (GRF)-family TFs is conserved in dicotyledons, and OsGRF3 and OsGRF10 have a repressive effect on OsKN2 in rice, resulting in reductions in plant internodes and increases in adventitious root numbers at nodes [29].

E. brevicornu is considered a traditional Chinese medicine with important commercial value; however, its seed dormancy has been a limiting factor for large-scale artificial cultivation. In this study, we optimized the method of seed dormancy release in *E. brevicornu*, compared the performance of seeds subjected to different stratification treatments in terms of embryo percentage and germination percentage, and explored the gene expression patterns under different stratification treatments using RNA-seq technology. We aimed to reveal the relationship between stratification treatment and seed dormancy and to explore the key genes that regulate seed dormancy in *E. brevicornu* in order to provide effective candidate genes and a theoretical basis for improving and creating nondormant superior *E. brevicornu* germplasm.

Results

A novel chill model applied to the dormancy release of *E. brevicornu* seeds

CU confirmation

E. brevicornu is a wide ecological amplitude plant. It occurs in the temperate and subtropical forests, thickets and slopes in China [30]. Plants bloom in May to June, and fruits mature from June to August. As seeds spread in summer, they would undergo high-low temperature changes until germination. Thus, we suggest, except for cold stratification, a variable-temperature process that simulates natural condition may also help to release physiological dormancy. So, we firstly monitor germination percentage in seeds in variable-temperature and low-temperature stratification.

As shown in Fig. 1, the germination percentage of *E. brevicornu* increased with an increasing number of days under each temperature treatment. At 4 °C, the final germination percentage of *E. brevicornu* seeds treated with chilling for 11 d was 15.56%, while the final germination percentage of *E. brevicornu* seeds treated with chilling for 104 d was 86.67%. This indicated that the dormancy-releasing effect of low temperature on *E. brevicornu* seeds accumulated gradually with increasing cold treatment days. The germination percentage reached a maximum of 86.67% after 104 d of chilling at a low temperature of 4 °C. The optimum temperature range was 2-6 °C. Within this temperature range, the final germination percentage of *E. brevicornu* seeds treated with chilling for 56 d was 84.44% at 4 °C, while the final germination percentage of seeds at 10 °C was only 33.33%. The slope of the curve for each treatment decreased significantly with increasing temperature, and the number of days required to reach the maximum germination percentage increased. During the same chilling treatment period of 104 d, *E. brevicornu* seeds took 1, 23, 49, 56, and 64 d to reach the maximum germination percentage under the treatments of 2, 4, 6, 8, and 10 °C, respectively.

Chilling unit can be used to describe the efficiency of each cold temperature on releasing seed dormancy and it was studied as follows. In this study, we took the relative slope value of the chilling-response curves (Fig. 1) at each temperature as the chilling unit value of each temperature (unit is CU). A CU model was constructed to describe the contribution of low temperature to the chilling unit. From Fig. 2A, the CU fitting function for the temperatures of 2, 4, and 6 °C was $Y = -0.1345X^2 + 1.0503X + 6.4583$ ($R^2 = 1$). The optimum temperature for *E. brevicornu* seed dormancy release was 3.90 °C, and the maximum CU was 8.5087.

We define the chilling accumulation for *E. brevicornu* seeds within an hour at a certain temperature as being equal to the chilling unit for the temperature. Then, the response curve of between chilling accumulation and the germination percentage was constructed, which we named CA model. Using this model, we can develop an accurate chilling strategy for the dormancy release of *E. brevicornu* seeds. The germination percentage was determined using the equation:

$$Germination\ percentage(\%) = \frac{A1 - A2}{1 + \left(\frac{X}{X0}\right)^P} - A2$$

where A1 and A2 are the minimum and maximum germination percentage achieved at a determined number of germination days, X0 is one-half of the CA required to achieve the maximum germination percentage, X is the chilling accumulation, and P is an equation-specific coefficient.

Figure 2B describes the CA model fitted by a logistic curve at the optimum cold-stratification temperature of 3.90 °C. The model describes the relationship between CA and germination percentage at 30, 40, 50, and 60 d of stratification, with R^2 values of 0.8856, 0.9254, 0.9206,

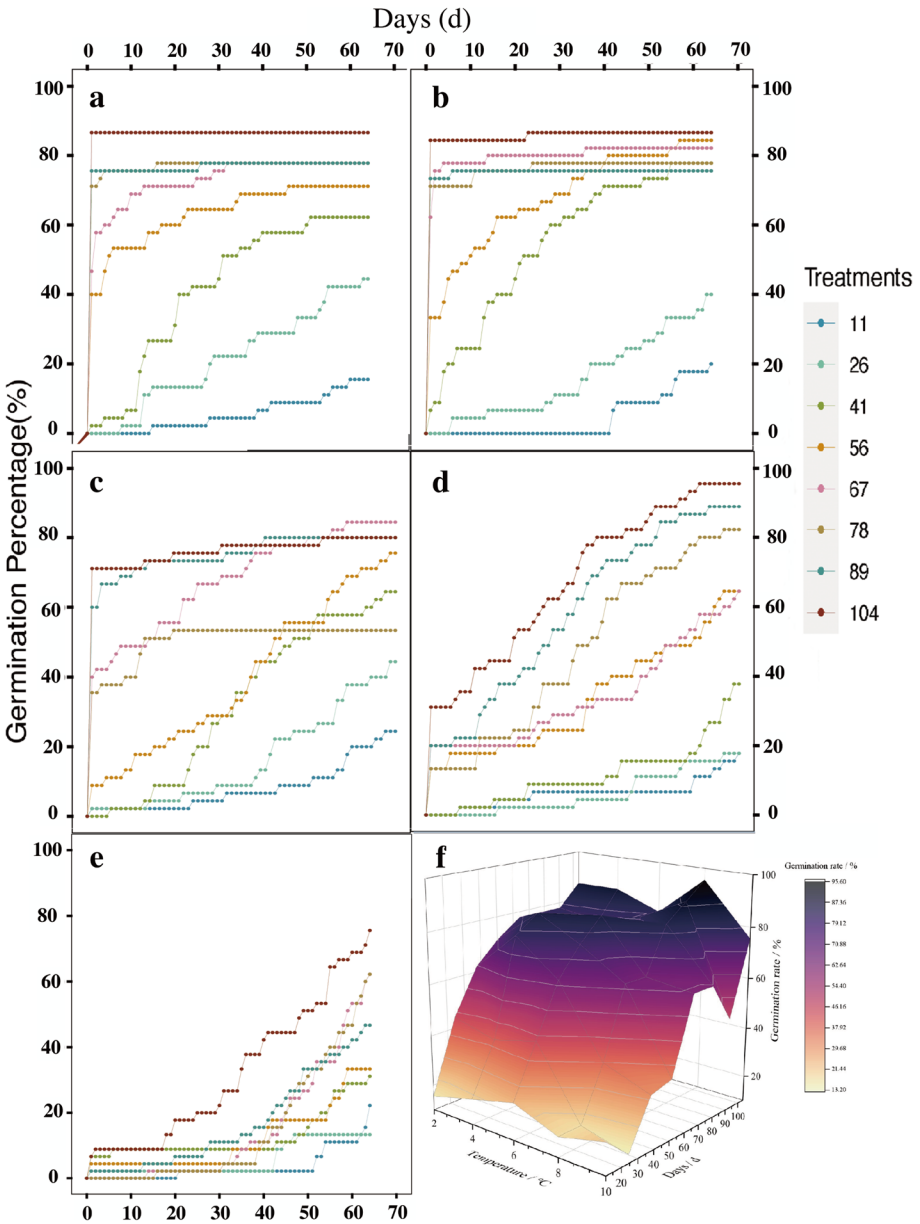

Fig. 1 Dynamic changes in *E. brevicornu* seed germination at different temperatures. **A**, **B**, **C**, **D**, and **E** are the germination percentages of seeds at 2, 4, 6, 8, and 10 °C, respectively; **F** shows the germination percentages of seeds over five temperature gradients

and 0.8907, respectively. From the figure, the X0 values at the four germination stages were 1005.6468 ± 100.5069, 806.6170 ± 57.1405, 763.3549 ± 42.5319, and 735.7646 ± 47.5271 CA. If the maximum germination percentage was reached at 30 d after stratification at 3.90 °C, the required stratification time was 2 × 1005.6468 CA/ 1 CU = 2011.2936 h. This resulted in the following CA values: 1613.234, 1526.7098 and 1471.5292 if the maximum germination percentage was reached at 40, 50, and 60 d after stratification at 3.90 °C.

Verification of the chilling models

The obtained CU and CA models were validated using *E. brevicornu* seeds from different harvesting years as experimental materials. As shown in Fig. 3A, R^2 = 0.8228 between the predicted and actual values of germination percentage, and the error band increased in width at low germination percentage (< 30%) and high germination percentage (> 60%), indicating that the CA model obtained by logistic fitting was less accurate in predicting lower versus higher germination

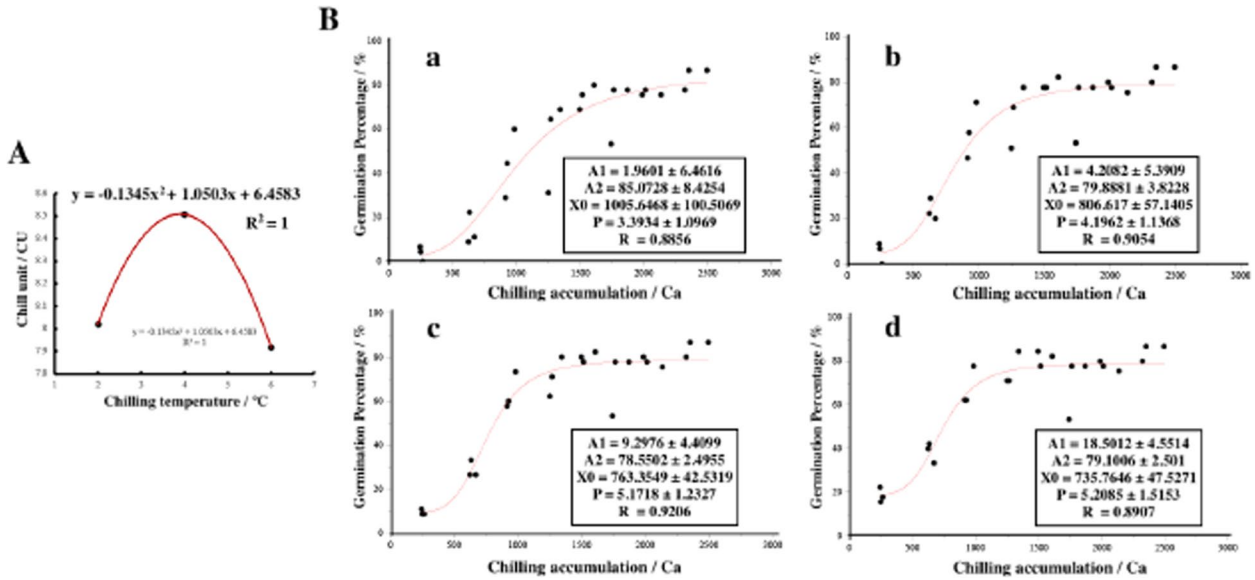

Fig. 2 Fitting of CU and CA. (A) Fitting of CU at each temperature. CU was fitted at temperatures of 2, 4, and 6 °C, and the best-fit temperature was 3.90 °C. (B) Logistic fitting of CA under different germination days. a, b, c and d show logistic fits of CA at 30, 40, 50, and 60 d of germination, respectively

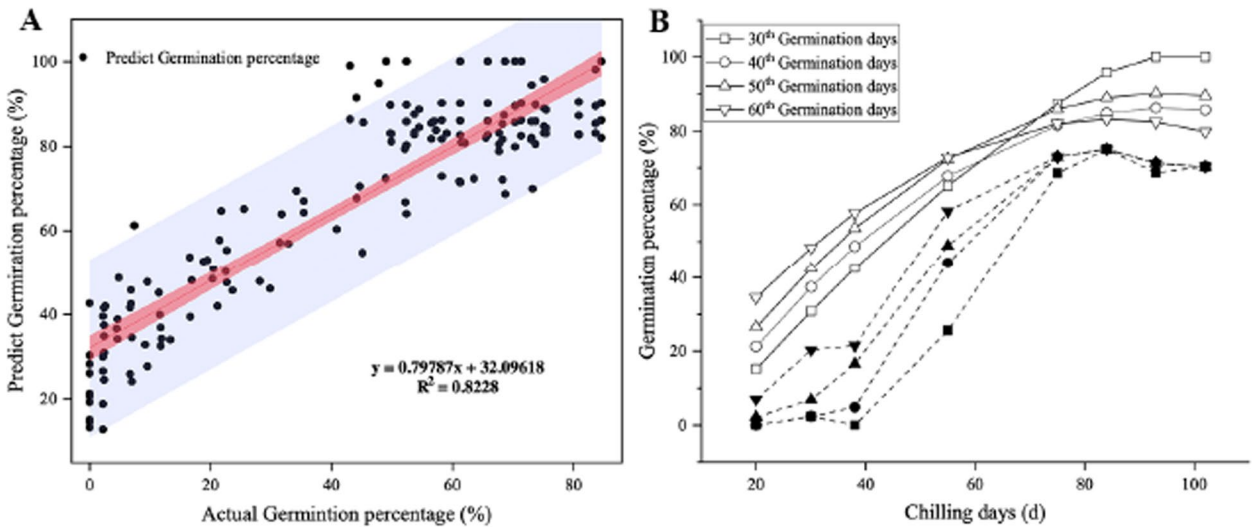

Fig. 3 Verification of chilling models in *E. brevicornu* seeds. **A** Correlation between predicted and actual germination percentage in the validation test of CA of *E. brevicornu* seeds. The red band is the error band, and the blue-purple band is the predicted bands. **B** Comparison of predicted and actual germination percentages after 30, 40, 50, and 60 d of germination at a temperature of 3.90 °C. Hollow shapes and solid shapes indicate predicted and actual values, respectively. Different geometric shapes indicate different germination days

percentage of *E. brevicornu* seeds. As shown in Fig. 3B, the actual germination percentages of *E. brevicornu* seeds after 30, 40, 50, and 60 d of stratification at the optimum temperature of 3.90 °C were lower than the predicted values.

Variable-temperature or low-temperature stratification alone did not contribute to the dormancy release of *E. brevicornu* seeds

As shown in Table 1, the embryo rate of *E. brevicornu* seeds without stratification treatment (0-0) was 6.77%,

Table 1 Effects of different variable-/low-temperature combination treatments on the embryo percentages of *E. brevicornu* seeds

Embryo percentage (%)		Low-temperature stratification time (m)				
		0	1	2	3	4
Variable-temperature stratification time (m)	0	6.77 ± 0.59	6.52 ± 1.10	13.54 ± 10.78	17.20 ± 9.43	18.21 ± 0.90
	1	7.44 ± 0.27	24.73 ± 28.07	24.84 ± 15.06	28.28 ± 17.20	40.27 ± 7.73
	2	21.45 ± 14.65	22.21 ± 5.61	35.01 ± 24.18	34.87 ± 11.97	47.10 ± 10.35
	3	9.96 ± 3.02	40.39 ± 22.36	36.71 ± 15.66	54.05 ± 15.22	57.95 ± 5.14
	4	17.70 ± 2.20	62.21 ± 6.65	87.01 ± 4.89	81.81 ± 12.71	91.68 ± 7.14

but the embryo rate reached 18.21% after 4 months of low-temperature stratification (0-4) and 17.7% after 4 months of variable-temperature stratification (4-0). The embryo rates of seeds after 2 months of variable-temperature stratification and 2 months of low-temperature stratification (2-2) or 1 month of variable-temperature stratification and 3 months of low-temperature stratification (1-3) were 35.01% and 40.39%, respectively. The embryo rate of seeds treated with 1-1 stratification increased from 7.44% to 24.73%, and that of seeds treated with 4-1 stratification increased from 17.70% to 62.21%. The seed embryos developed rapidly after the seeds were transferred from variable-temperature stratification to low-temperature stratification for 1 month. The results indicated that variable-temperature stratification and low-temperature stratification alone did not significantly contribute to seed embryo development and that a combination of variable-temperature and low-temperature stratification was required to release seed dormancy in *E. brevicornu*. To further investigate the effects of different stratification treatments on seed dormancy, we calculated the germination percentages of seeds under different treatments. Figure S1 shows the germination percentages of all variable-temperature-low-temperature stratification combinations at different temperature gradients. The germination percentage of *E. brevicornu* seeds in the 4-3 stratification combination was the highest among all temperature gradients, reaching 90.0% at 39 d under the 4 °C treatment, followed by the 3-3 and 2-3 stratification combinations.

Clustering analysis divided the nine treatment combinations into three major clusters according to transcriptome data (Fig. 4A). Cluster I included 1-3, 2-3, 3-3 and 4-2, cluster II included 4-1 and 4-3, cluster III included 4-0, 0-0, and 0-3. Three major groups were formed according to the growth status of the seed embryos with dashed lines (Fig. 4B). Group I included 4-0, 0-0, and 0-3, corresponding to Fig. 4B-a, B-b, and B-c, respectively. Group II included 1-3, 2-3, and 3-3, corresponding to Fig. 4B-d, B-e, and B-f, respectively. Group III included 4-1, 4-2, and 4-3, corresponding to Fig. 4B-g, B-h, and B-i, respectively. The results of transcriptome data clustering were not consistent with those of embryo percentage grouping. This indicated possible post-transcriptional and translational mechanisms of regulation of gene expression might exist here, which need further study.

Different seed structures can be distinguished through safranin O-fast green staining. Nonlignified cells appear green from fast green staining, and lignified cells appear magenta from safranin O staining. As seen from the figure, the proembryonal cells of *E. brevicornu* seeds in the 0-0, 0-3, and 4-0 treatments developed into globular embryos, still at the early stage of seed embryo development; the endosperm occupied the vast majority and clearly developed into two parts, with the part near the embryo being the small embryo cells (SEM) and most of the part away from the embryo differentiating into the large embryo cells (HEM) (Fig. 4Bb). In the microstructure of 1-3, 2-3, and 3-3 cotyledon embryos at the early stage (Fig. 4Be), the SEM inclusions gradually disappeared and formed a clear cavity, while the HEM inclusions remained clearly visible and the cotyledon (CO) started to develop. In the 4-2 and 4-3 treatments, most of the seed embryos developed to the late stage of cotyledon embryo or germination, and the microstructure showed that the SEM completely disappeared and degenerated into a layer of cells surrounding the embryo, the HEM cell layer thinned at the embryo root, and the cotyledons elongated further (Fig. 4Bh).

The first principal component (PC1) explained 16.617% of the characteristics of the original dataset, from which it was found that the 4-0 and 0-3 treatments (which involved only low- or variable-temperature stratification), as well as the control treatment (0-0), were significantly separated from the other treatments. The second principal component (PC2) explained 9.684% of the characteristics of the original dataset. According to the second principal component, the separation between the control treatment (0-0) and the other treatments was significant (Figure S2).

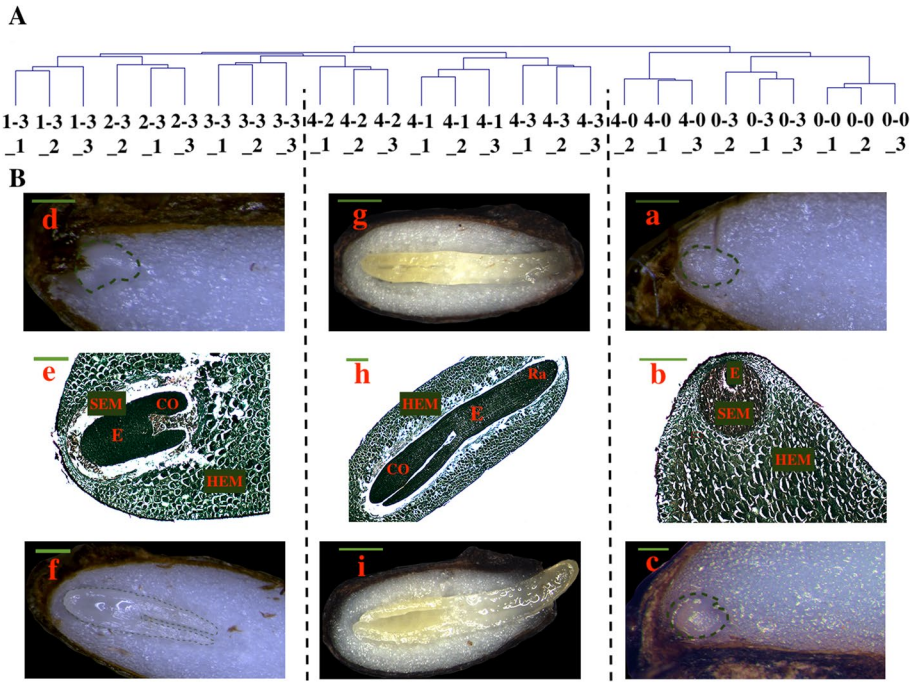

Fig. 4 Effect of stratification on *E. brevicornu* seeds. (A) Clustering analysis of differentially expressed genes among comparison groups. (B) Developmental statuses of *E. brevicornu* seed embryos with different stratification treatments. a. Globular embryo period, b. globular embryo microstructure, c. heart embryo period, d. torpedo embryo period, e. early cotyledon microstructure, f. mid-cotyledon embryo, g. late cotyledon embryo, h. late cotyledon embryo microstructure, i. germination; seed embryo stained with Safranin O-Fast Green stain. SEM: small endosperm cells; HEM: large endosperm cells; CO: cotyledon; Ra: radicle. The scale bar is 1 mm. The black dashed line shows the embryo phenotype at different stages according to embryo percentage, and the green dashed line shows the outline of embryo shapes

Transcriptome sequencing results reveal the dormancy release mechanism of *E. brevicornu* seeds

Differentially expressed gene (DEG) filtering

To investigate the dormancy release mechanism of *E. brevicornu* seeds under different stratification treatments, we selected nine treatments (0-0, 0-3, 1-3, 2-3, 3-3, 4-3, 4-2, 4-1, 4-0) for transcriptome sequencing, with three replicates per treatment, and seeds without stratification treatments were used as controls (0-0). In total, we obtained 191.54 Gb of clean data, and the data for each sample reached 6 Gb. The Q30 base percentage was at least 88%. These statistics suggested that the quality and amounts of the generated reads were sufficient for transcriptome analysis (Table S1). The clean data for 27 samples were assembled using Trinity, resulting in 513793 transcripts and 433387 unigenes. The N50 and mean length of the assembled transcripts were 794 bp and 575 bp, respectively. For the unigenes, the N50 and mean length were 884 bp and 637 bp, respectively (Table S2). A total of 71,990 DEGs ($|\log2(\text{fold change})| \geq 1$ and FDR < 0.05) were obtained by two-by-two comparisons of seeds from the nine stratification treatments of *E. brevicornu* (Figure S3).

To investigate the molecular mechanism of variable-temperature stratification on release from physiological dormancy in Epimedium, we selected five comparison groups, 0-0 vs. 4-0, 0-3 vs. 1-3, 0-3 vs. 2-3, 0-3 vs. 3-3, and 0-3 vs. 4-3, for which the total number of DEGs was 2525. To investigate the molecular mechanism of low-temperature stratification on release from physiological dormancy in Epimedium, we selected four comparison groups, 4-0 vs. 4-1, 4-0 vs. 4-2, 4-0 vs. 4-3, and 0-0 vs. 0-3, for which the total number of DEGs was 3340 (Fig. 5A).

To identify the biological pathways with which these DEGs may be associated, we annotated the 2525 and 3340 DEGs with the KEGG database (Fig. 5B). The DEGs in both comparison groups of variable temperature and low-temperature stratification were significantly enriched in plant hormone signal transduction (ko04075), starch and sucrose metabolism (ko00500), metabolic pathways (ko01100) and secondary metabolite biosynthesis (ko01110), and the results of the enrichment analysis imply the importance of plant hormone signal transduction and starch-sucrose metabolism pathways for the dormancy release of *E. brevicornu* seeds.

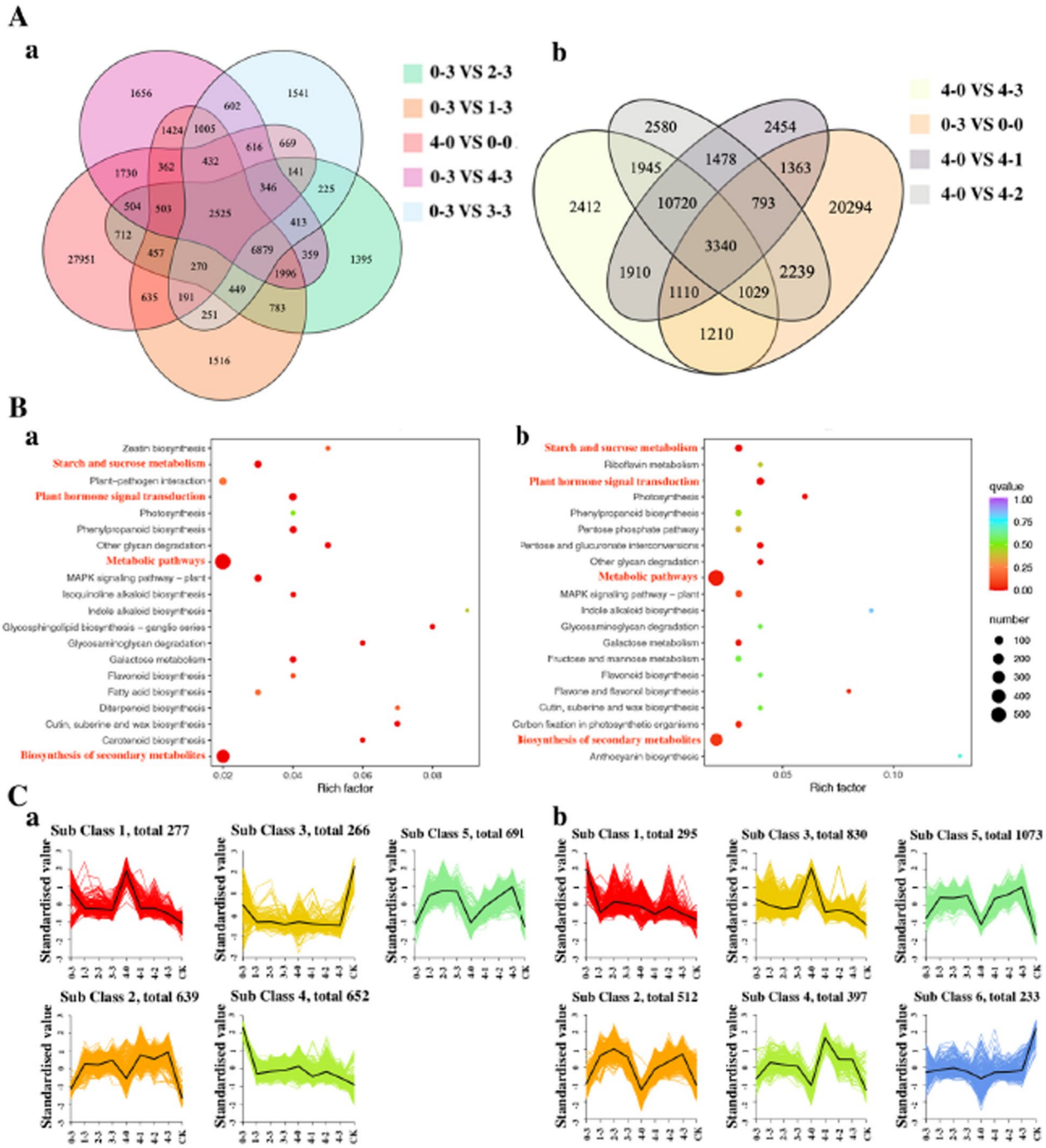

Fig. 5 Analysis of DEGs between variable-temperature stratification and low-temperature stratification groups. (A) Venn diagram analysis of DEGs. a. Venn diagram analysis of 5 variable-temperature stratification groups; b. Venn diagram analysis of 4 low-temperature stratification groups. (B) DEG KEGG enrichment analysis graph. a. KEGG enrichment analysis of 5 variable-temperature stratification groups; b. KEGG enrichment analysis of 4 low-temperature stratification groups. (C) K-means clustering analysis of DEGs. a. K-means clustering analysis of 5 variable-temperature stratification groups; b. K-means clustering analysis of 4 low-temperature stratification groups. The annotated genes were aligned against Kyoto Encyclopedia of Genes and Genomes (KEGG) (http://www.genome.jp/kegg/), and obtained the appropriate copyright permission to modify the KEGG image depicted in Fig. 5

By K-means clustering analysis, we obtained 5 and 6 clusters across samples in the two stratified comparison groups (Fig. 5C). Among them, clusters 2 and 5 showed the expected DEG accumulation pattern associated with the dormancy release of *E. brevicornu* seeds: the expression of DEGs gradually increased as the degree of dormancy diminished. Cluster 2 contained 1151 genes, and cluster 5 contained 1764 genes.

Analysis of plant hormone signal transduction and starch-sucrose metabolism pathways

Interestingly, gene expression in cluster 2 and cluster 5 increased with dormancy release, and the results of the enrichment analysis implied the importance of plant hormone signal transduction and starch-sucrose metabolism pathways for dormancy release in *E. brevicornu* seeds. Therefore, we performed a detailed analysis of phytohormone and starch-sucrose metabolism-related genes in cluster 2 and cluster 5.

The accumulation patterns of 1330 and 1585 DEGs detected in cluster 2 and cluster 5, respectively, were consistent with the degree of dormancy release in *E. brevicornu* seeds. Among them, 42 and 33 DEGs belonged to the plant hormone signal transduction pathway (Fig. 6A), and 40 and 32 DEGs belonged to the starch and sucrose metabolism pathway (Fig. 6B). A total of 42 significant DEGs were identified in plant hormone signal transduction pathways in the variable-temperature stratification group (Fig. 6A). Four enzyme-encoding genes, including the auxin transporter gene AUX1, the auxin receptor gene TIR1, the early auxin response gene AUX/IAA, and ARF, were identified in the IAA pathway. Three enzyme-encoding genes, including the histidine-containing phosphotransfer protein gene (AHP), a two-component response regulator ARR-B-family gene (B-ARR), and a two-component response regulator ARR-A-family gene (A-ARR), were identified in the cytokinin (CTK) pathway. DELLA was identified in the GA pathway. Two enzyme-encoding genes were identified in the ABA pathway, including the abscisic acid receptor PYR/PYL-family gene PYR/PYL and the PP2C gene. The gene encoding the enzyme mitogen-activated protein kinase

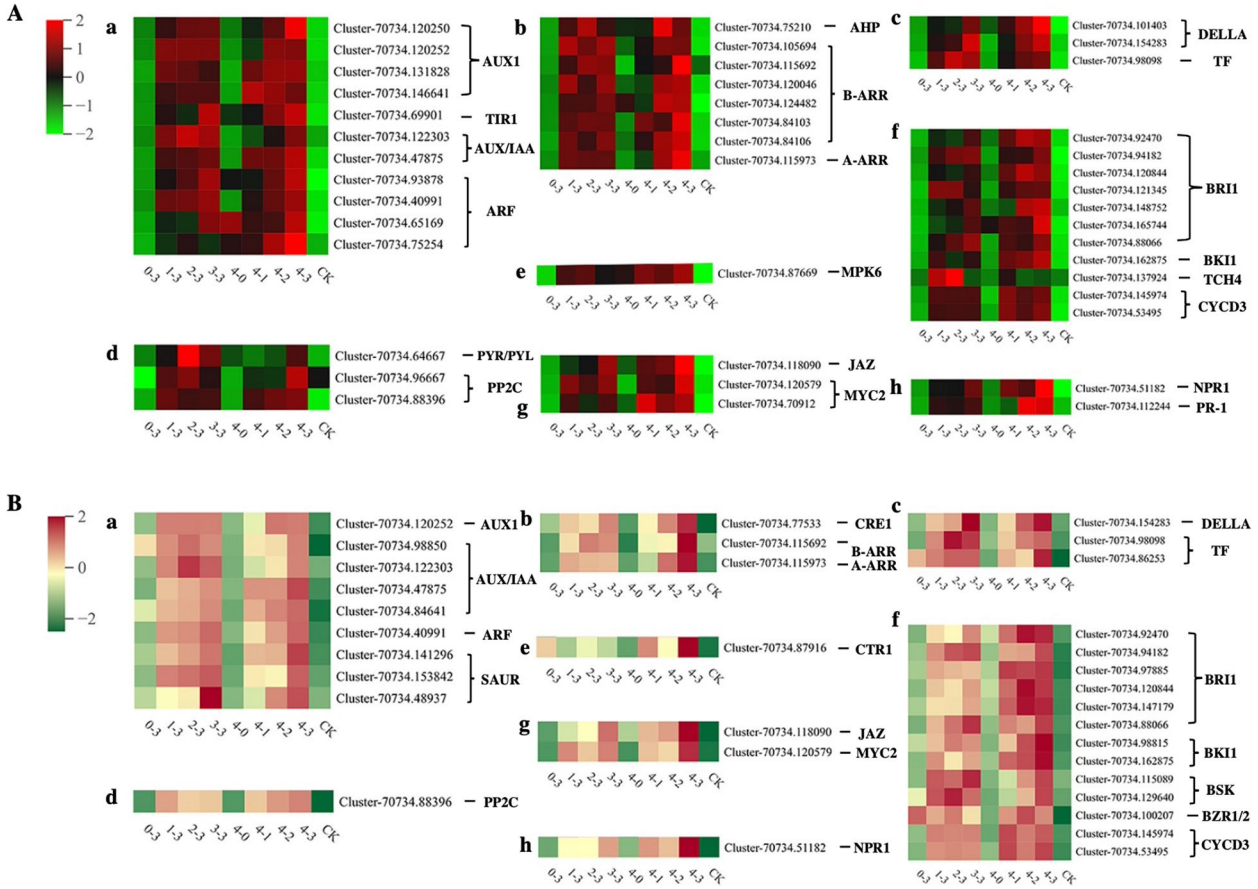

Fig. 6 Expression of each hormone-related transcript in *E. brevicornu* seeds of different treatment groups. (A) Expression of each hormone-related transcript in *E. brevicornu* seeds of the variable-temperature stratification group. (B) Expression of each hormone-related transcript in *E. brevicornu* seeds of the low-temperature stratification group. a. IAA; b. CTK; c. GA; d. ABA; e. ethylene; f. BR; g. JA; h. SA

6 (MPK6) was identified in the ethylene (Eth) pathway. Four enzyme-encoding genes, including BR-insensitive 1 (BRI1), BRI1 kinase inhibitor 1 (BKI1), TCH4, and cyclin D3 (CYCD3), were identified in the BR pathway. Two enzyme-encoding genes, including JA ZIM domain-containing protein (JAZ) and the TF MYC2, were identified in the JA pathway. Two enzyme-encoding genes, including the regulatory protein NPR1 and pathogenesis-related protein 1 (PR-1), were identified in the salicylic acid (SA) pathway.

A total of 33 significant DEGs were enriched in plant hormone signalling pathways in the low-temperature stratification group (Fig. 6B). Five enzyme-encoding genes whose expression differed in the low-temperature treatment compared to the variable-temperature treatment included ARF in the IAA pathway, the CTK receptor CRE1 in the CTK pathway, the serine/threonine-protein kinase CTR1 in the Eth pathway, and BR-signalling kinase (BSK) and brassinazole-resistant 1/2 (BZR1/2) in the BR pathway.

Sucrose is a synthetic precursor of starch in developing seeds [31]. The expression of genes related to starch and sucrose metabolic pathways is shown in Fig. 7. The morphological dormancy of *E. brevicornu* seeds was gradually released as the stratification time increased. Sucrose synthase (SUS, EC:2.4.1.13) in seeds is usually associated with starch accumulation and can indirectly promote relatively highly efficient starch biosynthesis by increasing the levels of the source of UDP-glucose (UDPG) [32, 33]. Meanwhile, glucose 6-phosphate is regulated by two enzymes, phosphoglucomutase (pgm, EC:5.4.2.2) and glucose-1-phosphate adenylyltransferase (glgC, EC:2.7.7.27), for the progressive synthesis of ADP-glucose (ADPG) and amylose. Increasing the concentrations of hexoses such as UDPG and ADPG induces the lengthening of long straight-chain starch chains by granule-bound starch synthase (WAXY, EC:2.4.1.242) and eventually by 1,4-α-glucan branching enzyme (glgB, EC:2.4.1.18), which synthesize amylose into starch, and the transcript levels of both enzymes were highest in the 4-3 treatment. During starch metabolism, the enzyme glycogen phosphorylase (glgP, EC:2.4.1.1) exerts feedback regulation, causing glycogen to be catabolized to α-glucose-1P upon accumulation of starch content.

Much glucose needs to be stored prior to starch synthesis to stimulate cell reproduction and delay differentiation [34], and as seed dormancy is released, glucose synthesis activity increases. UDPG generates 1,3-β-glucan as a major component of the cell wall via 1,3-β-glucan synthase, which in turn synthesizes glucose from glucan endo-1,3-β-D-glucosidase (EGLC, EC:3.2.1.39). The transcript expression of β-glucosidase gradually increased with the stratification time of *E. brevicornu* seeds and was highest under 4-3 stratification. The enzyme β-fructofuranosidase (SacA, EC:3.2.1.26) catabolizes sucrose directly into glucose, and its transcript level peaked under 2-3 stratification along with the dormancy release of *E. brevicornu* seeds. Starch was also decomposed with stratification time due to activation of isoamylase (ISA, EC:3.2.1.68) and α-amylase (AMY, EC:3.2.1.1) to produce soluble oligosaccharides, which were then instantly catabolized by β-amylase into maltose and eventually by the enzyme 4-α-glucanotransferase (malQ, EC:2.4.1.25) gene into glucose. As shown in the figure, β-amylase transcript levels remained low in the 4-0 treatment, verifying the speculation that a single

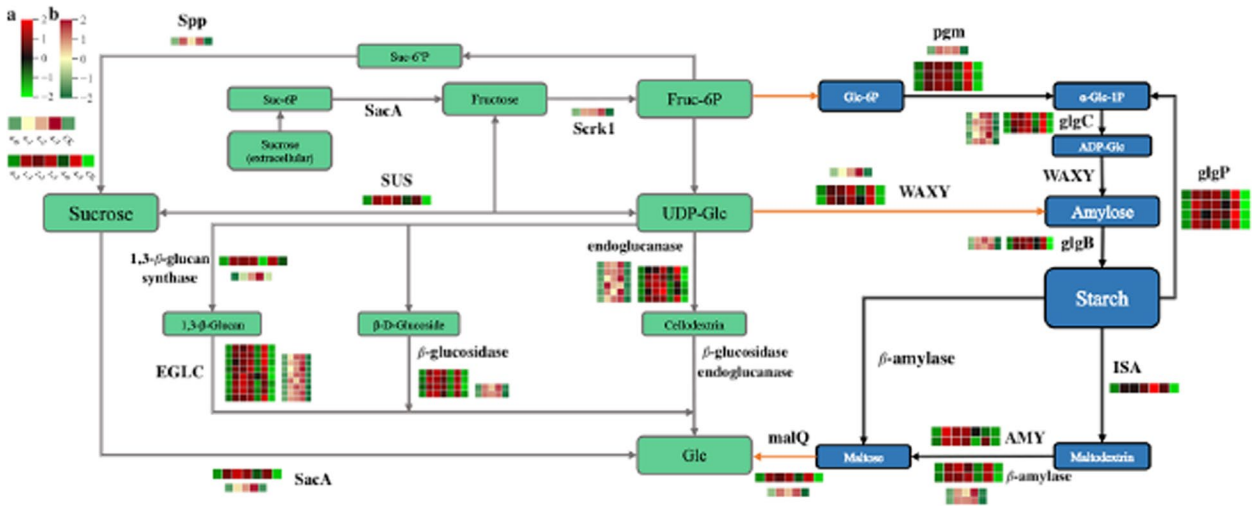

Fig. 7 Analysis of starch and sucrose metabolic pathways during dormancy release in *E. brevicornu* seeds. a. Differential expression analysis of 5 variable-temperature comparison groups; b. Differential expression analysis of 4 low-temperature comparison groups

variable-temperature stratification did not release the dormancy of *E. brevicornu* seeds.

Analysis of metabolic pathways of embryo development ending in seed dormancy and fatty acid degradation during dormancy

To explore more deeply and systematically the DEGs associated with the dormancy release of *E. brevicornu* seeds, we clustered 71990 DEGs, 57011 of which were excluded due to unclear expression patterns. The resulting total of 14979 genes are displayed in Fig. 5. These genes were divided into 17 clusters (Fig. 8A). Among them, clusters 1, 2, 3, 7, 11, 12, 13, 14, and 16 contained genes that were individually highly expressed in different stratification treatments, and cluster 5 contained genes that were coexpressed in the combined variable-temperature-low-temperature stratification. Fifteen of the 17 clusters were significantly enriched with genes, while cluster 12 and cluster 17 did not have significantly enriched genes (Fig. 8B). Cluster 2 contained the most

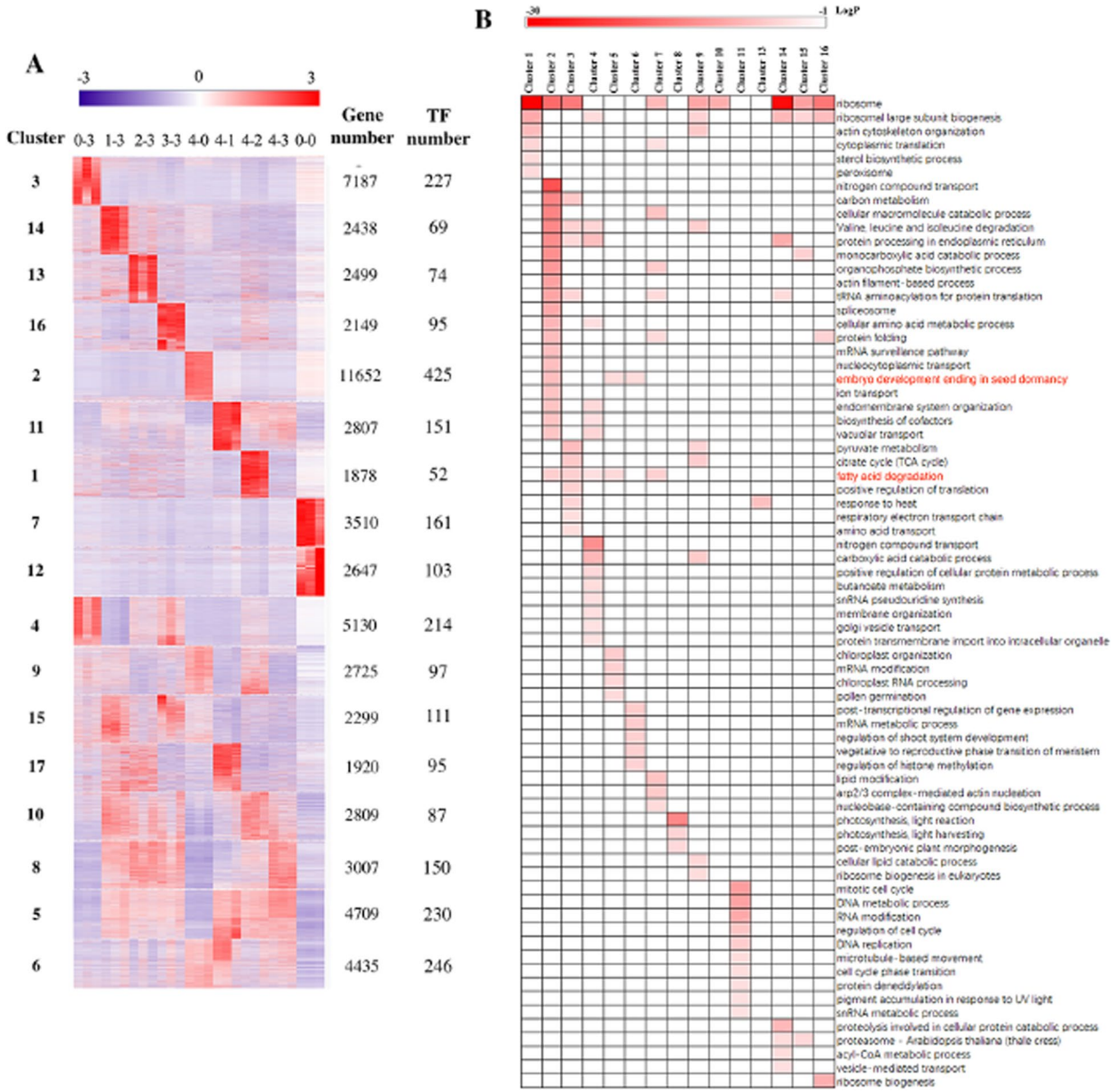

Fig. 8 DEG trend analysis and clustering heatmap. (A) Heatmap for differential gene expression trend analysis. The first column is the number of genes, and the second column is the number of TFs. (B) Term clustering heatmap

genes, which were individually highly expressed in the 4-0 treatment, while cluster 1 contained the fewest genes, which were individually highly expressed in the 4-2 treatment. Cluster 2 contained the most TFs, and cluster 1 contained the fewest TFs.

The genes in cluster 5 were co-highly expressed in the combined variable-temperature-low-temperature stratification. To illustrate the effect of combined stratification in relieving *E. brevicornu* seed dormancy, we analysed the biological pathways associated with cluster 5 and found that two pathways, embryo development ending in seed dormancy and fatty acid degradation, were significantly enriched.

As shown in Fig. 9A, a total of 35 genes associated with embryo development ending in seed dormancy (GO:000573) were selected. The transcript levels of these genes were significantly higher in the combination stratification than in the treatment groups that were treated only with low or variable temperature. Among them was BRI1, which senses and combines with BR; sterol 14α-demethylase (CYP51, EC:1.14.14.154), which is involved in the biosynthesis of phytosterols and BRs [35]; thiamine phosphate phosphatase (rsgA, EC:3.1.3.100), which is involved in the regulation of endogenous GA content and is commonly expressed in actively growing and elongating plant tissues [36]; 3-oxoacyl- synthase II (fabF, EC:2.3.1.179), which is associated with α-linolenic acid metabolism; pyruvate dehydrogenase E2 component (DLAT, EC:2.3.1.12), which is associated with the first step of fatty acid biosynthesis; and acyl-CoA oxidase (ACOX1, 3, EC:1.3.3.6), which is the main enzyme of the fatty acid β-oxidation pathway.

A total of six genes related to fatty acid degradation (ko00071) were filtered, as shown in Fig. 9B. Fatty acid degradation begins with long-chain acyl-CoA synthetase (ACSL, EC:6.2.1.3), which activates the transformation of free fatty acids into acyl-CoA; this step is followed by a β-oxidation cycle that serially breaks down acetate units [37]. The expression of alcohol dehydrogenase (adh, EC:1.1.1.1), which is involved in fatty acid β-oxidation, and ACOX1 was significantly higher in the combined stratification treatment groups (1-3, 2-3, 3-3, 4-1, 4-2, 4-3) than in the treatment groups that were stratified only by variable temperature or low temperature (0-3, 4-0) versus the control group (0-0) (Fig. 9B). Oxidation of hexadecanoic acid to acetyl-CoA, followed by butanoate metabolism, glyoxylate and dicarboxylate metabolism, and citrate metabolism pathways, provided energy for the dormancy release of *E. brevicornu* seeds (Fig. 9C).

Gene coexpression analysis

In this study, coexpression analysis of 4709 DEGs in cluster 5 with 230 TFs was performed to infer the reciprocal regulatory relationships between genes. To ensure strong interconnections among genes, the top 100 pairs of reciprocal relationships with absolute values of correlation coefficients ≥ 0.96 were screened for in-depth analysis.

Figure10 shows the core network of coexpression analysis, which included 11 TFs and 69 genes. In this network, GRF TFs had the most interactions, interacting with 12 genes. Next were BAF and MYB TFs, which interacted with 9 genes. The others were AUX/IAA and ARF, YABBY, C3H and KNOX, HD-Zip and zf-HD, and TCP, which had interactions with 8, 6, 5, 4, and 3 genes, respectively. The TFs zf-HD and YABBY also interacted with each other, as did MYB, GRF and TCP, with correlation coefficients greater than 0.98 (Figure S4).

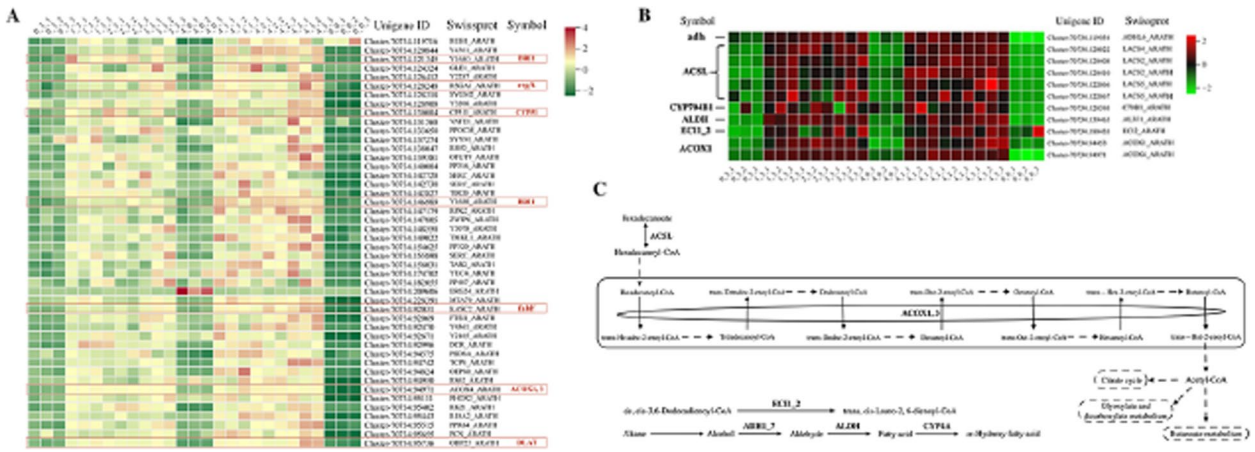

Fig. 9 DEG analysis of seed embryo growth and fatty acid degradation during dormancy in *E. brevicornu*. (A) DEG heatmap of seed embryo development ending in seed dormancy. (B) DEG heatmap of fatty acid degradation. (C) Analysis of fatty acid degradation metabolic pathways

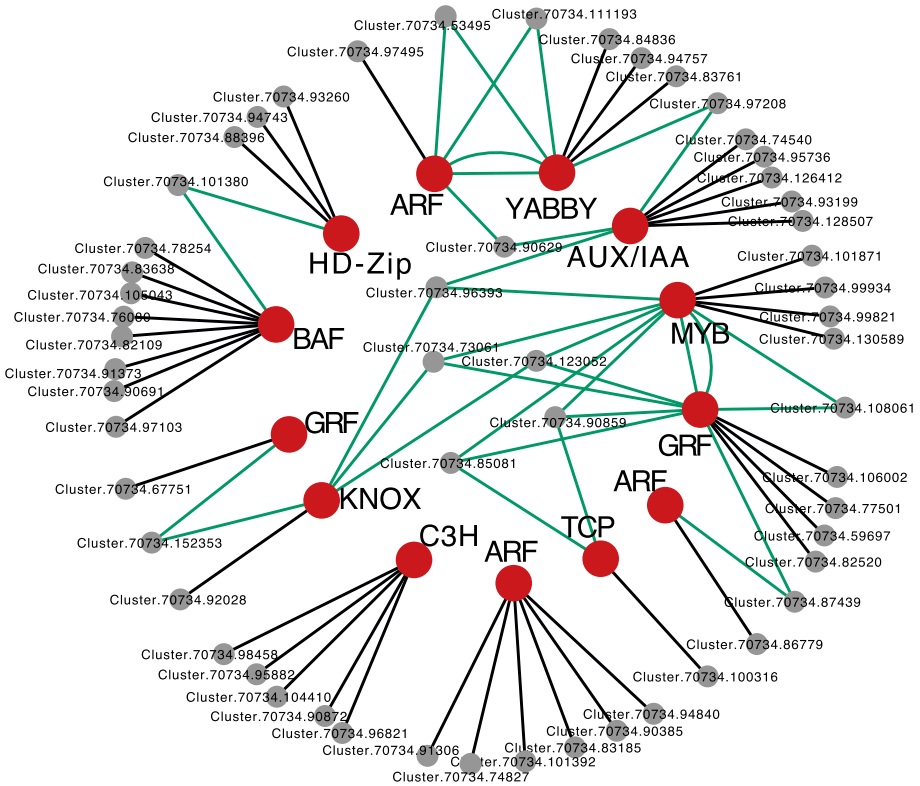

Fig. 10 Gene coexpression network in Cluster 5 with interactions between DEGs and TFs among them. The grey nodes represent the DEGs, and the red nodes represent the TFs that play a major role

Methods

Sampling and stratification

E. brevicornu seeds were sampled from May to August 2020 in Zhuoni County (Gannan Tibetan Autonomous Prefecture, Gansu Province, N34°30′53.75″, E103°34′28.60″). After artificially removing impurities and drying the seeds in the shade, seeds with full and uniform growth traits were selected and stored at 4 °C. Before stratification, the seeds were surface disinfected with 75% ethanol for 60 s and washed with distilled water. Then, the seeds were disinfected with 1% NaClO solution for 15 min. Finally, the seeds were rinsed under distilled water until no NaClO remained. The seed samples were stratified with 1:7 (v/v) wet sand (80% moisture content) in the germination box. The mixture was cultivated in a dark growth chamber at 10 °C/20 °C (12 h/12 h) for variable-temperature stratification for 0∼4 months and then transferred to 4 °C for low-temperature stratification for 0∼4 months (25 treatments in total).

Hereafter, the treatments are described as "months of variable-temperature stratification - months of low-temperature stratification (i.e., "4-3" indicates variable-temperature stratification for 4 months followed by low-temperature stratification for 3 months).

Chilling unit (CU) and chilling accumulation (CA) confirmation

After 4 months of variable-temperature stratification, seeds were placed in temperature-gradient seed germination beds with 3 mm of vermiculite substrate with a moisture content of 85%. The sterilized seeds were evenly placed on vermiculite at temperatures of 2, 4, 6, 8, and 10 °C, and each temperature gradient was repeated three times. The seeds were removed after 11, 28, 41, 56, 67, 78, 89, and 104 d of treatment; transferred to a 4 °C growth chamber; and observed daily for germination under dark conditions. The germination percentage was recorded daily for a total of 64 d. Germination was characterized by breakthrough of the seed coat by the radicle.

The final germination percentage at each temperature was used for polynomial fitting, and the relative value compared to the highest relative value in the fitted equation was named the chilling unit (CU), which was defined as the chill acquired over 1 h at that temperature. The fitted curve of the CU value under the temperature gradient was considered the CU model. The obtained CU at each temperature was substituted for each treatment to obtain the chilling accumulation (CA = CU * hour). The

response curve of CA versus germination percentage under different treatments was considered the CA model.

Verification of the chilling models

E. brevicornu seeds were sampled in July 2017 from Zhuoni County (Gannan Tibetan Autonomous Prefecture, Gansu Province, N34°30′53.75″, E103°34′28.60″) and placed in germination beds at 5 temperature gradients of 2, 3, 3.9, 5, and 6 °C, with 15 seeds per treatment; three replications were performed. The seeds of each treatment group of *E. brevicornu* were removed at 20, 30, 38, 55, 75, 84, 93, and 102 d and transferred to a 4 °C growth chamber. Seed germination was observed daily under dark conditions. The germination percentage was recorded daily for 64 d.

Measurement of the embryo length of seeds

Twenty seeds per treatment were randomly selected and then dissected longitudinally. Seed length and embryo length were measured using a Moticam 3000 (Motic China Group Co., Ltd.), and the embryo length:seed length ratio was calculated using the following formula:

$$Embryo\ ratio = Embryo\ length(cm)/Seed\ length(cm)$$

Observation of seed microstructure

Paraffin sectioning was used for microstructural observation of seeds [38]. Ten to twenty seeds in each treatment were immersed in formalin acetate alcohol (FAA) mixed fixative and vacuumed for 6~8 min. The samples were dehydrated in gradient ethanol and xylene, embedded in wax, and then sliced with a Leica RM2256 into 8 μm serial slices. Then, the slices were dewaxed in gradient xylenol and ethanol and stained with Safranin O-Fast Green. Finally, the sections were sealed with Canadian gum and then observed and photographed under an Olympus microscope.

RNA extraction and detection

E. brevicornu seeds from 4-0, 4-1, 4-2, 4-3, CK, 0-3, 1-3, 2-3, and 3-3, a total of nine treatment combinations, were selected as test materials. Ten to 15 seeds were randomly selected from the above treatments, immediately frozen in liquid nitrogen and stored at -80 °C until RNA extraction. Total RNA extraction was performed using an RNAprep Pure Plant Total RNA Extraction Kit (Tiangen), and each treatment was repeated three times.

Agarose gel electrophoresis was performed to analyse the sample RNA integrity and the presence of DNA contamination. A NanoPhotometer spectrophotometer was used to detect RNA purity (OD260/280 and OD260/230 ratio), and a Qubit 2.0 fluorometer was used to accurately quantify the RNA concentration. An Agilent 2100 bioanalyzer was used for accurate detection of RNA integrity.

Library preparation and transcriptome sequencing

A total amount of 1 μg of RNA per sample was used as input material for RNA library preparation. Sequencing libraries were generated using an NEBNext® Ultra^{TM} RNA Library Prep Kit for Illumin® (NEB, USA) following the manufacturer's recommendations, and index codes were added to attribute sequences to each sample. Briefly, mRNA was purified from total RNA using poly-T oligo-attached magnetic beads. Fragmentation was carried out using divalent cations under elevated temperature in NEBNext First Strand Synthesis Reaction Buffer (5X). First-strand cDNA was synthesized using random hexamer primers and M-MuLV Reverse Transcriptase (RNase H). Second strand cDNA synthesis was subsequently performed using DNA Polymerase I and RNase H. Remaining overhangs were converted into blunt ends via exonuclease/polymerase activity. After adenylation of the 3' ends of DNA fragments, NEBNext Adaptor with a hairpin loop structure was ligated to prepare for hybridization. To preferentially select cDNA fragments 250~300 bp in length, the library fragments were purified with an AMPure XP system (Beckman Coulter, Beverly, USA). Then, 3 pl of USER Enzyme (NEB, USA) was used with size-selected, adaptor-ligated cDNA at 37 °C for 15 min followed by 5 min at 95 °C before PCR. PCR was performed with Phusion High-Fidelity DNA polymerase, universal PCR primers, and Index (X) Primer. Finally, the PCR products were purified (AMPure XP system), and library quality was assessed on an Agilent Bioanalyzer 2100 system.

Clustering and sequencing

Clustering of the index-coded samples was performed on a cBot Cluster Generation System using a TruSeq E Cluster Kit v3-cBot-HS (Illumina) according to the manufacturer's instructions. After cluster generation, the library preparations were sequenced on an Illumina platform, and 150 bp paired-end reads were generated.

Data analysis

Fastp v0.19.3 was used to perform quality control on the raw data to generate clean reads. Trinity 2.11.0 was used to assemble transcripts from the clean reads. The coding sequences (CDSs) of the transcripts obtained by Trinity assembly were predicted using TransDecoder (https://github.com/TransDecoder/) to obtain the amino acid sequences corresponding to the transcripts. The redundant transcript sequences were compared with the Kyoto Encyclopedia (KEGG), Nonredundant (NR), Swiss-Prot, Gene Ontology (GO), Clusters of Orthologous Groups

(COG)/euKaryotic Orthologous Groups (KOG) and Trembl databases using DIAMOND, and the amino acid sequences were compared with the Pfam database using HMMER to obtain the transcripts for gene function annotation. The expression of transcripts was calculated using RSEM, and then the fragments per kilobase of transcript per million mapped reads (FPKM) value of each transcript was calculated based on the transcript length. Differential expression analysis between the two groups was performed using DESeq2 v1.22.1, and the *P* value was corrected by the Benjamini & Hochberg method. The fixed *P* values as well as the |log2(fold change)| values were used as thresholds for significant differential expression. Enrichment analysis was performed based on the hypergeometric test; for KEGG analysis, hypergeometric distribution tests were performed to identify pathways, while for GO analysis, the tests identified GO terms. Gene coexpression analysis results were plotted using Cytoscape v3.9.1.

Discussion

Role of IAA in the dormancy release of *E. brevicornu* seeds

Auxins play key roles in major aspects of plant growth and developmental processes, including apical dominance, tropic responses, vascular differentiation, embryo patterning, and root-and-shoot structuring [39]. Auxin regulates cell elongation by inducing rapid acidification of the cell wall, affecting the activity of ion channels for cell expansion and affecting the expression and activity of genes encoding cell wall components [40, 41].

Aux/IAA plays a central role in auxin signalling [42]. Two Aux/IAA proteins have been reported to be involved in seed development in Arabidopsis [43]. Transcript accumulation of many GmIAA genes has also been detected at various stages of soybean seed development (globular-stage [Gs] seeds, heart-stage [Hs] seeds, and cotyledon-stage [Cs] seeds) [44]. The interaction of ARFs and Aux/IAA is a key regulator of auxin-regulated gene expression [45]. Intracellular IAA stimulates the activity of ARFs, whose DNA-binding domains bind to and regulate the expression of auxin-responsive elements (AuxREs) in the Aux/IAA and small auxin-upregulated RNA (SAUR) promoters [46, 47]. In addition to auxin, various other hormones regulate SAUR expression, such as BR, GA, and ABA. SAUR participates in auxin-regulated cell elongation and expansion through an acid growth mechanism by inhibiting the activity of the type 2C protein phosphatase (PP2C) family and thereby regulating the PM H-ATPase phosphorylation state [48]. The transcript levels of multiple SAUR genes increased with increasing time of variable-temperature stratification, suggesting that SAUR may be a key gene by which variable-temperature stratification releases seed dormancy in E. brevicornu. At low concentrations of auxin, Aux/IAA inhibits the auxin response by binding to ARF, leading to repression of the target ARF TF. Direct binding of IAA to TIR1 promotes the interaction between SCF^{TIR1} and Aux/IAA to degrade AUX/IAA, which releases ARF [39, 49]. ARF10 and ARF16 are required for the formation of the root cap in a redundant pattern [50]. Seven ZmARF genes (ZmARFs 1, 10, 13, 14, 18, 22, and 25) are constitutively expressed in the developing embryo, suggesting that maize ARF genes may be involved in seed development and germination [51]. Therefore, we suggest that the interactions among the auxin signalling pathway components (ARF, AUX/IAA, SAUR and TIR1) relieve the dormancy of *E. brevicornu* seeds during stratification.

The interaction of IAA with ABA is necessary to maintain seed dormancy. ABA acts through the PYR/RCAR-PP2C-SnRK2 signalling cascade [52]. ABA-insensitive 3 (ABI3), a major component downstream of ABA signalling, is activated by ARF10/16 to stimulate ABA signalling and thus control seed dormancy [53]. Although PYR/PYL and PP2C transcript levels were increased, whether the increases indicate that cascade signalling is used to maintain *E. brevicornu* seed dormancy during stratification requires further investigation.

Roles of BRs in the dormancy release of E. brevicornu seeds

BRs help to promote seed germination and control the direction and rate of cell division [54, 55]. In addition, BRs have been shown to have additional nontranscriptional effects on vascular organization, thereby altering the mechanical properties of the cell wall [56]. BRs are also involved in the regulation of carbohydrates [57].

BRI1 is involved in cell division and elongation as a restricted and conserved component of the BR-binding complex [58]. In rice, OsBRI1 participates in organ development through the control of cell division and elongation [54]. GhBRI1 mRNA expression is significantly higher in rapidly elongating cells of cotton hypocotyls than in mature roots [59]. BRs reverse the inhibition of seed germination by ABA and exhibit an accessory function in the promotion of cell expansion and seed germination by GAs [60]. In the current study, the transcript level of CYP51, also identified as being involved in embryo development ending in seed dormancy entry, was significantly higher in the combined stratification than in the variable-temperature or low-temperature stratification and peaked in the 4-3 treatment (Fig. 9A). CYP51 encodes obtusifoliol 14α-demethylase, an enzyme involved in the synthesis of phytosterols [61]. Sterols are structural components of cell membranes and act as biosynthetic precursors of BRs, playing important roles in membrane fluidity and permeability [62]. It has been shown that CYP51G1-Sc functions as a biologically active

signalling lipid molecule in embryogenesis and that most of the seed embryos of Arabidopsis mutant plants stop developing at an early heart-type embryo stage [63].

When the BR content is high, BRs are sensed and bound by BRI1. This activates the BRI1/BAK1 kinase complex, thereby inhibiting downstream blockers of BR signalling, including the GSK3-like kinase protein BR-insensitive 2 (BIN2, EC:2.7.11.1). Inhibition of BIN2 leads to the accumulation of nonphosphorylated BZR1/2-family TFs that regulate the expression of BR target genes [64]. Gallego et al. [65] showed that the physical interaction between BZR1 and DELLAs is the molecular basis of BR-GA crosstalk, and it has been found that BZR1 promotes seed germination by accelerating endosperm rupture via promotion of cell elongation in the plumular axis-radicle transition zone. The levels of several BKI1 transcripts in *E. brevicornu* seeds increased with increasing stratification time, and although BKI1 is a negative regulator of BR signalling whose activity is maintained at a low level, some studies have shown that this low activity still allows the expression of BR biosynthetic genes [66].

Role of energy (starch and fatty acid) supply in the dormancy release of *E. brevicornu* seeds

Mobilization of energy reserves is essential for seed germination. Energy is stored mostly in the form of lipids and starch in the embryos of dicotyledons. In cereals, mainly amylases and glucanases digest the starch present in the endosperm to form glucosyl that serves as the energy source for seed germination [67]. In rape seeds, both starch and lipids are synthesized in the plastid, and the degradation of starch provides the nearest carbon source for the rapid synthesis of lipids [68]. Lipids are mostly present in dicotyledons as triacylglycerols (TAGs), which provide the carbon skeleton and energy for seed development through fatty acid oxidation, the glyoxylate cycle, the partial tricarboxylic acid cycle, and gluconeogenesis [69]. The mitochondrial pyruvate dehydrogenase complex (mtPDC) is the main entry point for carbon into the tricarboxylic acid cycle, catalysing the oxidative decarboxylation of pyruvate to produce acetyl-CoA, CO2, and NADH, with DLAT forming its core structure [70]. Yu et al. [71] reported reduced carbon flux into the TCA cycle in m132, an Arabidopsis DLAT mutant, which resulted in severely diminished ATP production and disrupted cell division. ACSL is a key regulator of fatty acid β-oxidation located in the peroxisome that is involved in seed dormancy release and germination processes [72]. A total of five ACSL transcripts during *E. brevicornu* stratification were highly expressed in the combined stratification group but weakly expressed in the low-temperature stratification (0-3) and variable-temperature stratification (4-0) groups, suggesting that combined stratification better stimulates fatty acid β-oxidation to provide energy for seed dormancy release (Fig. 9B).

Roles of TF interactions in the dormancy release of E. brevicornu seeds

Two sets of reciprocal regulatory relationships among putative genes had correlation coefficients greater than 0.98: 1) zf-HD and YABBY and 2) MYB, GRF, and TCP (Figure S4). The homology domain (HD) family participates in plant and animal development by regulating protein-protein interactions and other domains/motifs with regulatory functions [73]. zf-HD is involved in plant development and stress responses, and its expression is also significantly correlated with Eth, ABA, and MeJA [74, 75]. Both TCP and GRF positively affect cell expansion and proliferation [76, 77]. The transcript levels of GRFs are usually negatively regulated by miR396, and TCP4 directly regulates miRNA396 to influence the expression levels of certain GRFs to regulate different cell proliferation pathways [78, 79]. Direct interactions between TCP and MYB TFs may lead to functional redundancy [80]. AtTCP14 is expressed in the vascular tissue of the seed radicle; this protein induces the expression of germination-related genes and activates the growth potential of the seed embryo [25]. MYB activates lignin biosynthesis in fibres and/or vessels, regulates the deposition of the cell wall components cellulose and xylan, and has been shown to play a role in the ABA signalling cascade as a positive regulator of the ABA response during seed germination [81, 82]. The interaction of TCP3 with R2R3-MYBs increases the flavonol content and negatively regulates the auxin response, resulting in a decrease in auxin content and transport ability [83]. Auxin has a limiting effect on seed germination, and its content gradually decreases with the gradual release of dormancy [84, 85]. Therefore, we speculate that the interaction among the three TFs may play a role in restricting IAA transport during seed stratification in *E. brevicornu*, leading to dormancy release, after which cell proliferation leads to seed embryo elongation that is accompanied by cell wall disintegration and results in seed germination.

Conclusion

We have revealed the regulatory mechanisms of sucrose and starch metabolism, plant hormone signalling, embryo development, and fatty acids in the dormancy release process of *E. brevicornu* seeds. In addition, our gene coexpression analysis revealed possible interactions between sugar and hormone signalling, providing new insights into the mechanism of dormancy release in *E. brevicornu* seeds.

Supplementary Information

The online version contains supplementary material available at https://doi.org/10.1186/s12870-024-05471-0.

Supplementary Material 1.

Supplementary Material 2.

Supplementary Material 3.

Supplementary Material 4.

Supplementary Material 5.

Supplementary Material 6.

Acknowledgements
Not applicable.

Authors' contributions
P.L.; validation, P.L., X.Q., and Y.W.; formal analysis, P.L.; investigation, P.L.; data curation, P.L.; writing-original draft prepa- ration, P.L.; writing-review and editing, X.D., and Y.W. All the authors reviewed the draft. All the author(s) have read and approved the final manuscript.

Funding
This work was funded by the Shandong Province Science and Technology enterprises Innovation Ability Improvement Project of Shandong Province (2022TSGC2062), National Natural Science Foundation of China (82104344).

Availability of data and materials
The 16S rDNA Illumina libraries obtained from the sequencing company were deposited at the NCBI's small read archive (SRA) in BioProject ID: PRJNA977838.

Declarations

Ethics approval and consent to participate
All methods were in compliance with relevant institutional, national, and international guidelines and legislation.

Consent for publication
Not applicable.

Competing interests
The authors declare no competing interests.

Received: 5 August 2023 Accepted: 30 July 2024
Published online: 08 August 2024

References

1. Zhuang W, Sun N, Gu C, Liu S, Zheng Y, Wang H, et al. A literature review on Epimedium, a medicinal plant with promising slow aging properties. Heliyon. 2023;9(11):e21226.
2. Yang L, Zhou S, Hou Y, Ji B, Pei L, Su X, et al. Blue light induces biosynthesis of flavonoids in *Epimedium sagittatum* (Sieb.et Zucc.) Maxim. leaves, a study on a light-demanding medicinal shade herb. Ind Crops Prod. 2022;187:115512.
3. Bentsink L, Koornneef M. Seed dormancy and germination. Arab B. 2008;6:e0119.
4. Baskin CC, Baskin JM. Seeds: Ecology, Biogeography, and Evolution of Dormancy and Germination. 2nd ed. San Diego: Academic Press; 2014.
5. Hao D. Study on methods of breaking dormancy and seedling cultivation of *Epimedium brevicornu* Maxim. seeds. Beijing: China Agricultural University; 2019.
6. Su H. A study about dormancy mechanisms and dormancy releasing methods in *Epimedium wushanense* (Berberidaceae) seed. Beijing: China Agricultural University; 2016.
7. Baskin CC, Baskin JM. A classification system for seed dormancy. Seed Sci Res. 2004;14:1–16.
8. Hang Y. Study of embryonic dormancy in seeds of *Kalopanax septemlobus*. Thunb. Koidz. J Northeast For Univ (Chin Ed). 1986;1:39–44.
9. Wang J, Liu P, He L, Jia L, Zeng Z, Lu J. Factors affecting seed germination in *Epimedium koreanum* Nakai. J Shenyang Pharm Univ. 2013;30(10):807–11.
10. Liu Y, Müller K, El-Kassaby YA, Kermode AR. Changes in hormone flux and signaling in white spruce (*Picea glauca*) seeds during the transition from dormancy to germination in response to temperature cues. BMC Plant Biol. 2015;18:592.
11. Ma Y, Chen X, Guo B. Identification of genes involved in metabolism and signalling of abscisic acid and gibberellins during *Epimedium pseudowushanense* B.L.Guo seed morphophysiological dormancy. Plant Cell Rep. 2018;37:1061–75.
12. Borisjuk L, Walenta S, Rolletschek H, Mueller KW, Wobus U, Weber H. Spatial analysis of plant metabolism: sucrose imaging within *Vicia faba* cotyledons reveals specific developmental patterns. Plant J. 2002;29:521–30.
13. Edelmann HG, Fry SC. Effect of cellulose synthesis inhibition on growth and the integration of xyloglucan into pea internode cell walls. Plant Physiol. 1992;100:993–7.
14. Xu W, Purugganan MM, Polisensky DH, Antosiewicz DM, Fry SC, Braam J. Arabidopsis TCH4, regulated by hormones and the environment, encodes a xyloglucan endotransglycosylase. Plant Cell. 1995;7:1555–67.
15. Müller K, Tintelnot S, Leubner MG. Endosperm-limited Brassicaceae seed germination: abscisic acid inhibits embryo-induced endosperm weakening of Lepidium sativum (cress) and endosperm rupture of cress and Arabidopsis thaliana. Plant Cell Physiol. 2006;47:864–77.
16. Leubner MG, Meins F. Sense transformation reveals a novel role for class I β-1,3-glucanase in tobacco seed germination. Plant J. 2000;23:215–21.
17. Wu CT, Leubner MG, Meins FJ, Bradford KJ. Class I beta-1,3-glucanase and chitinase are expressed in the micropylar endosperm of tomato seeds prior to radicle emergence. Plant Physiol. 2001;126:1299–313.
18. Marowa P, Ding Y, Kong A. Expansins: roles in plant growth and potential applications in crop improvement. Plant Cell Rep. 2016;35:949–65.
19. Yanagisawa S. Transcription factors in plants: physiological functions and regulation of expression. J Plant Res. 1998;111:363–71.
20. Liu L, White MJ, MacRae TH. Transcription factors and their genes in higher plants functional domains, evolution and regulation. Eur J Biochem. 1999;262:247–57.
21. Zhang Y, Cao G, Qu LJ, Gu H. Characterization of Arabidopsis MYB transcription factor gene AtMYB17 and its possible regulation by LEAFY and AGL15. J Genet Genomics. 2009;36:99–107.
22. Li L, Yu X, Thompson A, Guo M, Yoshida S, Asami T, et al. Arabidopsis MYB30 is a direct target of BES1 and cooperates with BES1 to regulate brassinosteroid-induced gene expression. Plant J. 2009;58:275–86.
23. Shin R, Burch AY, Huppert KA, Tiwari SB, Murphy AS, Guilfoyle TJ, et al. The Arabidopsis transcription factor MYB77 modulates auxin signal transduction. Plant Cell. 2007;19:2440–53.
24. Yang SW, Jang IC, Henriques R, Chua NH. FAR-RED ELONGATED HYPOCOTYL1 and FHY1-LIKE associate with the Arabidopsis transcription factors LAF1 and HFR1 to transmit phytochrome A signals for inhibition of hypocotyl elongation. Plant Cell. 2009;21:1341–59.
25. Tatematsu K, Nakabayashi K, Kamiya Y, Nambara E. Transcription factor AtTCP14 regulates embryonic growth potential during seed germination in Arabidopsis thaliana. Plant J. 2008;53:42–52.
26. Schommer C, Palatnik JF, Aggarwal P, Chételat A, Cubas P, Farmer EE, et al. Control of jasmonate biosynthesis and senescence by miR319 targets. PLoS Biol. 2008;6:e230.
27. Sugio A, Kingdom HN, MacLean AM, Grieve VM, Hogenhout SA. Phytoplasma protein effector SAP11 enhances insect vector reproduction by manipulating plant development and defense hormone biosynthesis. Proc Natl Acad Sci USA. 2011;108:e1254-1263.
28. Laosatit K, Amkul K, Yimram T. A Class II KNOX gene, KNAT7-1, regulates physical seed dormancy in mungbean [*Vigna radiata* (L.) Wilczek]. Front Plant Sci. 2022;13.
29. Kuijt SJ, Greco R, Agalou A, Shao J, Hoen CC, Overnäs E, et al. Interaction between the GROWTH-REGULATING FACTOR and KNOTTED1-LIKE HOMEOBOX families of transcription factors. Plant Physiol. 2014;164:1952–66.

30. Ying J, Boufford DE, Brach AR. Flora of China, vol. 19. Beijing and St. Louis: Science Press and Missouri Botanical Garden Press; 2011.
31. Smith AM, Denyer K, Martin C. The synthesis of the starch granule. Annu Rev Plant Physiol. 1997;48:67–87.
32. Weschke W, Panitz R, Sauer N, Wang Q, Neubohn B, Weber H, et al. Sucrose transport into barley seeds: molecular characterization of two transporters and implications for seed development and starch accumulation. Plant J. 2000;21:455–67.
33. Cao H, He M, Zhu C, Yuan L, Dong L, Bian Y, et al. Distinct metabolic changes between wheat embryo and endosperm during grain development revealed by 2D-DIGE-based integrative proteome analysis. Proteomics. 2016;16:1515–36.
34. Díaz-Granados VH, López-López JM, Flores-Sánchez J, Olguin-Alor R, Bedoya-López A, Dinkova TD, et al. Glucose modulates proliferation in root apical meristems via TOR in maize during germination. Plant Physiol Biochem. 2020;155:126–35.
35. Lin Y, Zhang C, Lan H, Gao S, Liu H, Liu J, et al. Validation of potential reference genes for qPCR in maize across abiotic stresses, hormone treatments, and tissue types. PLoS ONE. 2014;9:901–15.
36. Fukazawa J, Sakai T, Ishida S, Yamaguchi I, Kamiya Y, Takahashi Y. Repression of shoot growth, a bZIP transcriptional activator, regulates cell elongation by controlling the level of gibberellins. Plant Cell. 2000;12:901–15.
37. Hayashi H, De Bellis L, Hayashi Y, Nito K, Kato A, Hayashi M, Hara-Nishimura I, Nishimura M. Molecular characterization of an Arabidopsis acyl-coenzyme a synthetase localized on glyoxysomal membranes. Plant Physiol. 2002;130:2019–26.
38. Li ZL. Plant tissue section production technology. 1st ed. Beijing: Science Publishers; 1987.
39. Quint QM, Gray WM. Auxin signaling. Curr Opin Plant Biol. 2006;9:448–53.
40. Hager A. Role of the plasma membrane H + -ATPase in auxin-induced elongation growth: historical and new aspects. J Plant Res. 2003;116:483–505.
41. Cosgrove DJ, Li LC, Cho HT, Hoffmann-Benning S, Moore RC, Blecker D. The growing world of expansins. Plant Cell Physiol. 2002;43:1436–44.
42. Woodward AW, Bartel B. Auxin: regulation, action, and interaction. Ann Bot. 2005;95:707–35.
43. Ploense SE, Wu MF, Nagpal P, Reed JW. A gain-of-function mutation in IAA18 alters Arabidopsis embryonic apical patterning. Development. 2009;136:1509–17.
44. Singh VK, Jain M. Genome-wide survey and comprehensive expression profiling of Aux/IAA gene family in chickpea and soybean. Front Plant Sci. 2015;27:918.
45. Weijers D, Benkova E, Jäger KE, Schlereth A, Hamann T, Kientz M, et al. Developmental specificity of auxin response by pairs of ARF and Aux/IAA transcriptional regulators. EMBO J. 2005;24:1874–85.
46. Ulmasov T, Hagen G, Guilfoyle TJ. ARF1, a transcription factor that binds to auxin response elements. Science. 1997;276:1865–8.
47. Tiwari SB, Hagen G, Guilfoyle T. he roles of auxin response factor domains in auxin-responsive transcription. Plant Cell. 2003;15:533–43.
48. Spartz AK, Ren H, Park MY, Grandt KN, Lee SH, Murphy AS, et al. SAUR Inhibition of PP2C-D Phosphatases Activates Plasma Membrane H+-ATPases to Promote Cell Expansion in Arabidopsis. Plant Cell. 2014;26:2129–42.
49. Kepinski S, Leyser O. The Arabidopsis F-box protein TIR1 is an auxin receptor. Nature. 2005;17:2204–16.
50. Wang JW, Wang LJ, Mao YB, Cai WJ, Xue HW, Chen XY. Control of root cap formation by MicroRNA-targeted auxin response factors in Arabidopsis. Plant Cell. 2005;17:2204–16.
51. Xing H, Pudake RN, Guo G, Xing G, Hu Z, Zhang Y, et al. Genome-wide identification and expression profiling of auxin response factor (ARF) gene family in maize. BMC Genomics. 2011;12:178.
52. Hubbard KE, Nishimura N, Hitomi K, Getzoff ED, Schroeder JI. Early abscisic acid signal transduction mechanisms: newly discovered components and newly emerging questions. Genes Dev. 2010;24:1695–708.
53. Liu X, Zhang H, Zhao Y, Feng Z, Li Q, Yang HQ, et al. Auxin controls seed dormancy through stimulation of abscisic acid signaling by inducing ARF-mediated ABI3 activation in Arabidopsis. Proc Natl Acad Sci USA. 2013;110:15485–90.
54. Nakamura A, Fujioka S, Sunohara H, Kamiya N, Hong Z, Inukai Y, et al. The role of OsBRI1 and its homologous genes, OsBRL1 and OsBRL3, in rice. Plant Physiol. 2006;140:580–90.
55. Hu Y, Yu D. BRASSINOSTEROID INSENSITIVE2 interacts with ABSCISIC ACID INSENSITIVE5 to mediate the antagonism of brassinosteroids to abscisic acid during seed germination in Arabidopsis. Plant Cell. 2014;26:4394–408.
56. Muñoz FJ, Labrador E, Dopico B. Brassinolides promote the expression of a new Cicer arietinum beta-tubulin gene involved in the epicotyl elongation. Plant Mol Biol. 1998;37:807–17.
57. Goetz M, Godt DE, Roitsch T. Tissue-specific induction of the mRNA for an extracellular invertase isoenzyme of tomato by brassinosteroids suggests a role for steroid hormones in assimilate partitioning. Plant J. 2000;22:515–22.
58. Wang ZY, Seto H, Fujioka S, Yoshida S, Chory J. BRI1 is a critical component of a plasma-membrane receptor for plant steroids. Nature. 2001;410:380–3.
59. Sun Y, Fokar M, Asami T, Yoshida S, Allen RD. Characterization of the brassinosteroid insensitive 1 genes of cotton. Plant Mol Biol. 2004;54:221–32.
60. Steber CM, McCourt P. A role for brassinosteroids in germination in Arabidopsis. Plant Physiol. 2001;125:763–9.
61. Xia K, Ou X, Tang H, Wang R, Wu P, Jia Y, et al. Rice microRNA osa-miR1848 targets the obtusifoliol 14α-demethylase gene OsCYP51G3 and mediates the biosynthesis of phytosterols and brassinosteroids during development and in response to stress. New Phytol. 2015;208:790–802.
62. Hartmann MA, Benveniste P. Plant membrane sterols: isolation, identification and biosynthesis. Methods Enzymol. 1987;148:632–50.
63. O'Brien M, Chantha SC, Rahier A, Matton DP. Lipid signaling in plants. Cloning and expression analysis of the obtusifoliol 14alpha-demethylase from Solanum chacoense Bitt., a pollination- and fertilization-induced gene with both obtusifoliol and lanosterol demethylase activity. Plant Physiol. 2015;139:734–49.
64. Kim TW, Wang ZY. Brassinosteroid signal transduction from receptor kinases to transcription factors. Annu Rev Plant Biol. 2010;61:681–704.
65. Zhong C, Patra B, Tang Y, Li X, Yuan L, Wang X. A transcriptional hub integrating gibberellin-brassinosteroid signals to promote seed germination in Arabidopsis. J Exp Bot. 2021;72:4708–20.
66. Wang X, Chory J. Brassinosteroids regulate dissociation of BKI1, a negative regulator of BRI1 signaling, from the plasma membrane. Science. 2006;313:1118–22.
67. Dekkers BJ, Schuurmans JA, Smeekens SC. Glucose delays seed germination in Arabidopsis thaliana. Planta. 2004;218:579–88.
68. Da Silva PF, Eastmond PJ, Hill LM. Starch metabolism in developing embryos of oil seed rape. Planta. 1997;203:480–7.
69. Eastmond PJ, Graham IA. Re-examining the role of the glyoxylate cycle in oilseeds. Trends Plant Sci. 2001;6:72–8.
70. Li-Beisson Y, Shorrosh B, Beisson F, Andersson MX, Arondel V, Bates PD, et al. Acyl-lipid metabolism. Arabidopsis Book. 2013;11:e0161.
71. Yu H, Du X, Zhang F, Hu Y, Liu S, Jiang X, et al. A mutation in the E2 subunit of the mitochondrial pyruvate dehydrogenase complex in Arabidopsis reduces plant organ size and enhances the accumulation of amino acids and intermediate products of the TCA cycle. Planta. 2012;236:387–9.
72. Liu S, Jiang X, Liu Z. Mechanism of the Breaking of Seed Dormancy by Flower Thinning in Heracleum moellendorffii Hance. J Plant Growth Regul. 2019;38:870–82.
73. Bürglin TR. A Caenorhabditis elegans prospero homologue defines a novel domain. Trends Biochem Sci. 1994;19:70–1.
74. Wang W, Wu P, Li Y, Hou X. Genome-wide analysis and expression patterns of ZF-HD transcription factors under different developmental tissues and abiotic stresses in Chinese cabbage. Mol Genet Genomics. 2016;291:1451–64.
75. Abu-Romman S. Molecular cloning and expression analysis of zinc finger-homeodomain transcription factor TaZFHD1 in wheat. S Afr J Bot. 2014;91:32–6.
76. Nicolas M, Cubas P. TCP factors: new kids on the signaling block. Curr Opin Plant Biol. 2016;33:33–41.
77. Kim JH, Lee BH. GROWTH-REGULATING FACTOR4 of Arabidopsis thaliana Is required for development of leaves, cotyledons, and shoot apical meristem. J Plant Biol. 2006;49:463–8.
78. Rodriguez RE, Mecchia MA, Debernardi JM, Schommer C, Weigel D, Palatnik JF. Control of cell proliferation in Arabidopsis thaliana by microRNA miR396. Development. 2010;137:103–12.

79. Schommer C, Debernardi JM, Bresso EG, Rodriguez RE, Palatnik JF. Repression of cell proliferation by miR319-regulated TCP4. Mol Plant. 2014;7:1533–44.
80. Spanudakis E, Jackson S. The role of microRNAs in the control of flowering time. J Exp Bot. 2014;65:365–80.
81. Zhou J, Lee C, Zhong R, Ye ZH. MYB58 and MYB63 are transcriptional activators of the lignin biosynthetic pathway during secondary cell wall formation in Arabidopsis. Plant Cell. 2009;21:248–66.
82. Reyes JL, Chua NH. ABA induction of miR159 controls transcript levels of two MYB factors during Arabidopsis seed germination. Plant J. 2007;49:592–606.
83. Li S, Zachgo S. TCP3 interacts with R2R3-MYB proteins, promotes flavonoid biosynthesis and negatively regulates the auxin response in Arabidopsis thaliana. Plant J. 2013;76:901–13.
84. Chao WS, Doğramacı M, Horvath DP, Anderson JV, Foley ME. Comparison of phytohormone levels and transcript profiles during seasonal dormancy transitions in underground adventitious buds of leafy spurge. Plant Mol Biol. 2017;94:281–302.
85. Sorce C, Lorenzi R, Ceccarelli N, Ranalli P. Changes in free and conjugated IAA during dormancy and sprouting of potato tubers. Funct Plant Biol. 2000;27:371–7.

Publisher's Note